Induced polarization and electronic properties of carbon-doped boron nitride nanoribbons

J. Beheshtian,[1] A. Sadeghi,[2] M. Neek-Amal,[1,3,*] K. H. Michel,[3] and F. M. Peeters[3]
[1]*Department of Physics, Shahid Rajaee Teacher Training University, Lavizan, Tehran 16785-136, Iran*
[2]*Department of Physics, Basel University, Klingelbergestrasse 82, CH-4056 Basel, Switzerland*
[3]*Departement Fysica, Universiteit Antwerpen, Groenenborgerlaan 171, B-2020 Antwerpen, Belgium*
(Received 22 April 2012; revised manuscript received 6 November 2012; published 29 November 2012)

The electronic properties of boron nitride nanoribbons (BNNRs) doped with a line of carbon atoms are investigated using density functional calculations. By replacing a line of alternating B and N atoms with carbons, three different configurations are possible depending on the type of the atoms which bond to the carbons. We found very different electronic properties for these configurations: (i) the NCB arrangement is strongly polarized with a large dipole moment having an unexpected direction, (ii) the BCB and NCN arrangements are nonpolar with zero dipole moment, (iii) the doping by a carbon line reduces the band gap regardless of the local arrangement of the borons and the nitrogens around the carbon line, and (iv) the polarization and energy gap of the carbon-doped BNNRs can be tuned by an electric field applied parallel to the carbon line. Similar effects were found when either an armchair or zigzag line of carbon was introduced.

DOI: 10.1103/PhysRevB.86.195433 PACS number(s): 62.25.−g, 71.15.Mb, 77.65.−j

I. INTRODUCTION

Single-layer hexagonal boron nitride (h-BN) nanosheets have been recently produced and placed on top of a SiO_2 substrate.[1] Several experimental groups have also fabricated free-standing h-BN single layers using sputtering of controlled energetic electron beams.[2,3] Unlike graphene, a h-BN sheet is a wide-gap insulator, as is hexagonal BN, which is a promising material for optoelectronic technologies,[4,5] tunnel devices, and field-effect transistors.[6,7] Small flakes of h-BN, i.e., BN nanoribbons (BNNRs), are semiconductors when hydrogen passivated on one of the edges.[8–10] The band gap of BNNR can be tuned by using different types of atoms for edge passivation.[11–14] The hybridized distributed domains of h-BN and C atoms have attracted much experimental and theoretical attention because of promising band-gap engineered applications in electronics and optics.[15,16] The zigzag BNNR has half-metallic properties when the boron edge is hydrogen passivated and the nitride edge is bare.[11] Under a hydrogen-rich environment, the zigzag BNNR with two hydrogen-terminated edges becomes a ferromagnetic metal.[14] Moreover, the electronic and magnetic properties of the BNNRs could be modulated by applying an extra transversal electric field. Zhang *et al.* used the local density approximation (LDA) to study the energy gap and showed that it can be tuned by applying a transverse electric field on semi-infinite hydrogen-passivated BNNRs with zigzag or armchair edges.[9] Similarly, by using the LDA, Park *et al.* found that a transverse electric field decreases the band gap of armchair BNNRs monotonically, while the band gap of zigzag BNNRs either increases or decreases depending on the direction and the strength of the applied field.[10] Additionally, random doping BN with C atoms leads to spontaneous magnetization.[17,18] Sai *et al.* found piezoelectricity in a heteropolar nanotube depending on the chirality and diameter of the nanotube which originates from the piezoelectric response of an isolated planar BN sheet.[19]

In this study, we report first-principles calculations for the BNNRs which are doped by a *zigzag line of carbon atoms* in the middle and passivated by hydrogen atoms at the edges. We study different possible positions of the line of carbon atoms with respect to the BN lattice and found that piezoelectricity and consequently the permanent polarization in the BNNRs can be strongly enhanced, tuned, or even eliminated depending on the type of atoms (B or N) that surround the dopants. We found that doping BNNRs by carbon atoms decreases the band gap, while the electric polarization of the doped BNNRs depends on the types of atoms (B or N) that surround the dopants. The NCB system is polarized in an unexpected way while BCB and NCN have zero dipole moments. Similar effects were found when (i) different widths of nanoribbons were used in the calculations, and (ii) an armchair line of carbons was put in the middle. We show that an external planar electric field applied along the C line either reduces or increases the band gap and the dipole moment depending on its direction.

II. MODEL AND METHOD

Figure 1 shows a sketch of long armchair boron nitride nanoribbons where a transverse electric field is applied through the long electrodes. In our simulation, a finite-size supercell is used as shown by the rectangle in the figure. The dangling bonds generated at the edges are saturated by hydrogen atoms. An electric field is applied parallel to the C line along which our system has a finite length. Notice that in the horizontal direction the system may be considered infinite (i.e., as nanoribbon, see next section).

We take a sheet $L \times W = 3.1 \times 3.4$ nm^2 in size as a perfect finite nanoribbon (see Fig. 2). The total number of B and N atoms in the sheet is 418; in addition, there are 56 H atoms at the edges. A zigzag line of 28 C atoms is inserted in the middle of the system replacing a line of h-BN atoms. We have studied three different positions of the carbon line (C line) with respect to the BN lattice as illustrated in Figs. 2(b)–2(d) and compare the results with the undoped sheet [Fig. 2(a)]. There are three different ways of inserting the central (zigzag) C line: (i) a C line in the center with boron atoms on one side and nitrogen atoms on the other side [Fig. 2(b)], which we name "NCB," (ii) a C line in the center with boron atoms on both

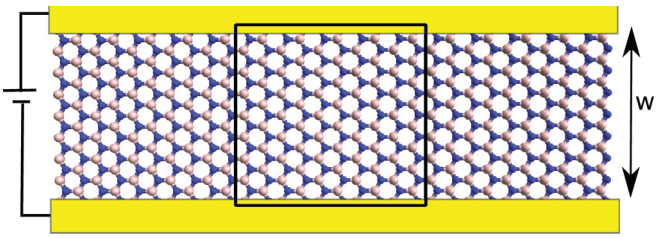

FIG. 1. (Color online) Sketch of a long armchair boron nitride nanoribbon subject to a transverse electric field imposed by the biased supporting electrodes (yellow strips). The width of the ribbon W is determined by the number of armchair lines. The rectangle shows the supercell used in our simulation.

sides [Fig. 2(c)], which we name "BCB," and (iii) a C line in the center with nitrogen atoms on both sides [Fig. 2(d)], which we name "NCN." Notice that all these systems are passivated by hydrogen atoms at the edges to saturate the edge chemical bonds.

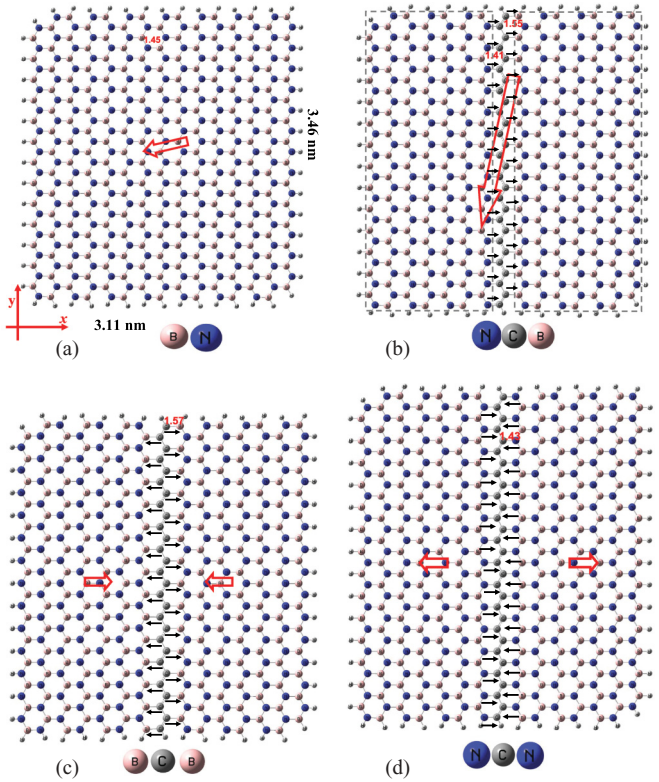

FIG. 2. (Color online) (a) Perfect boron nitride nanoribbon (BN). (b) Boron nitride nanoribbon with a zigzag C line in the middle surrounded by both boron and nitrogen atoms on both sides (NCB). (c) Boron nitride nanoribbons with the C line surrounded only by boron atoms on both sides (BCB). (d) Boron nitride nanoribbons with the C line surrounded only by nitrogen atoms on both sides (NCN). In (a) and (b), red arrows refer to the total dipole moment of the systems and in (c) and (d), red arrows refer to the total dipole moment on the two sides. The black horizontal arrows refer to the local dipoles corresponding to the B-C or N-C bonds. The size of the simulated system is 3.46×3.11 nm^2 (Fig. 2). Numbers refer to the bond lengths in Å unit.

We employ density functional theory as implemented in GAUSSIAN (G09) (Ref. 20) which is an electronic-structure package that uses a basis set of Gaussian type of orbitals. For the exchange-correlation (XC) functional, the hybrid functional B3LYP is adopted in G09. For some particular cases, we also used the LDA as implemented in the BIGDFT package,[21] which uses real-space wavelets. In both cases, the self-consistency loop iterates until the change in the total energy is less than 10^{-7} eV, and the geometries are considered relaxed once the force on each nucleus is less than 50 meV/Å. Using the 6-31G* basis set in G09, we expect that our calculation is capable to provide a reliable description of the electronic properties of the different systems. Natural bonding orbital (NBO) analysis[22] is also performed at the B3LYP/6-31G* level of theory.[20]

III. RESULTS

A. Effect of finite length and H saturation

Before we present the main results of this paper, we estimate the effects of both the finite size along the axis of the ribbon and the presence of the hydrogens at the edges. We performed DFT calculations using B3LYP for an infinitely long (i.e., periodic along the ribbon axis) pristine BN nanoribbon. The unit cell contains two atomic lines with the same width as the BN system and a k-point mesh of $12 \times 1 \times 1$. Results for the energy eigenvalues (for nanoribbon with infinite length and finite width W) at the center of the Brillouin zone together with the results for finite-size ribbon with length L and width W are depicted in Fig. 3. Note that the band gap for the infinite ribbon is slightly larger, but the difference is small, i.e., 7%. Therefore, we assume that the H-saturated edges of the finite samples have only a small effect on the energy gap throughout this work.

Applying periodic boundary conditions along the ribbon axis is computationally straightforward only for a pure ribbon (without the C line).The other studied systems (e.g., NCB) have a strong dipole line in the center of the nanoribbon.

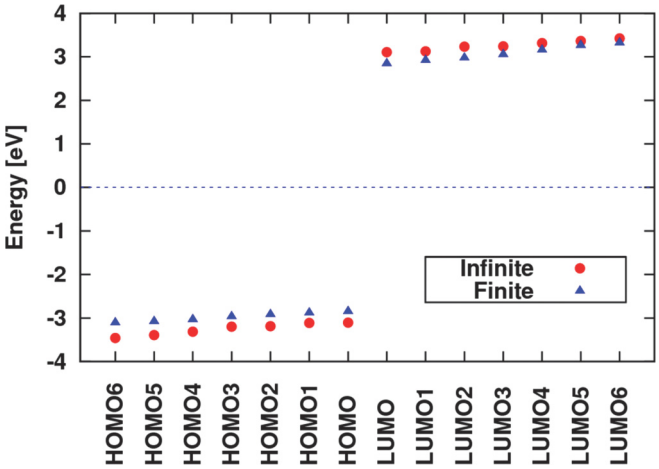

FIG. 3. (Color online) Energy eigenvalues close to the Fermi level (set to 0) for finite (blue) and infinitely long (red) BN nanoribbons with the same width. In both cases, the DFT calculations were performed with the B3LYP functional. For the infinite BN, only the energy eigenvalues at the center of the Brillouin zone are shown.

TABLE I. Bond lengths in Å, HOMO–LUMO energy gap in units of eV, and spontaneous electric-dipole moment P_0 in units of Debye for the four (three) studied nanoribbons with a zigzag (armchair) C line inserted as shown in Fig. 2 (Figs. 10 and 11). Results for the gap are given from B3LYP calculations.

Nanoribbon	$d_{B\text{-}N}$	$d_{B\text{-}C}$	$d_{N\text{-}C}$	$d_{C\text{-}C}$	Gap	P_o
Zigzag C line						
BN	1.45				5.69	10.8
NCB	1.45	1.55	1.41	1.40	1.52	44.24
BCB	1.45	1.57		1.46	1.47	0.08
NCN	1.45		1.43	1.39	1.47	0.27
Armchair C line						
BN	1.45				5.69	11.97
NCB	1.45	1.52	1.42	1.43	1.71	1.72
NCN	1.46	1.51	1.4	1.44	1.99	10.70

Because of the long-range nature of the electrostatic interactions, one needs a very long periodicity length in order to ensure that the interaction between periodic images of the dipole line are negligible. In order to reduce the computational demands, we will restrict ourselves to samples, albeit rather long.

B. Lattice mismatch

We recall that in bulk h-BN, the in-plane B-N bond length $d_{BN} = 1.446$ Å was determined by x-ray scattering.[23] Previous *ab initio* calculations[24] yielded $d_{BN} = 1.437$ Å while we obtained $d_{BN} = 1.45$ Å. On the other hand, the bond lengths d_{NC} and d_{BC} between the inserted C-line atoms and the N and B surrounding atoms, as well as the intrachain bond length d_{CC} between C atoms, depend on the specific configuration of the atoms in the NCB, BCB, and NCN systems (see Fig. 2). We summarized the results of our calculations in Table I. We found for the three doped BNNRs that $d_{CC} < d_{BN} < d_{BC}$. Notice that the relative sheet bond lengths $d_{NC} = 1.41$ and 1.43 Å in NCB and NCN, respectively, are an indication of the partially double-bond character of the N-C bonds at the central C line which is remarkable. The difference in bond lengths around the C line in NCB is clearly visible in Fig. 2(b). A typical lattice mismatch, due to inserting C line, for NCB system is depicted in Fig. 4. The values $d_{BC} = 1.55$ Å and $d_{NC} = 1.41$ Å lead to a lattice mismatch and symmetry breaking between the left and the right parts of our system along the inserted C line. Notice that we did not observe considerable out-of-plane movement due to the carbon insertion. This is not surprising because both graphene and BN sheets have planar sp^2 hybridization.

C. Electronic charge distribution

The perfect infinite BN sheet is a neutral sheet with a uniform charge distribution far from the edges. Indeed, in an infinite two-dimensional h-BN sheet, the point-group symmetry is D_{3h} and there is no permanent dipole moment. However, in finite BNNR structures, the symmetry is broken which allows piezoelectricity, i.e., the appearance of a dipole under mechanical deformation. Therefore, the h-BN sheet is the most simple crystalline structure which allows piezoelectricity.[25,26] On the other hand, in BNNRs the finite extension of the sheet

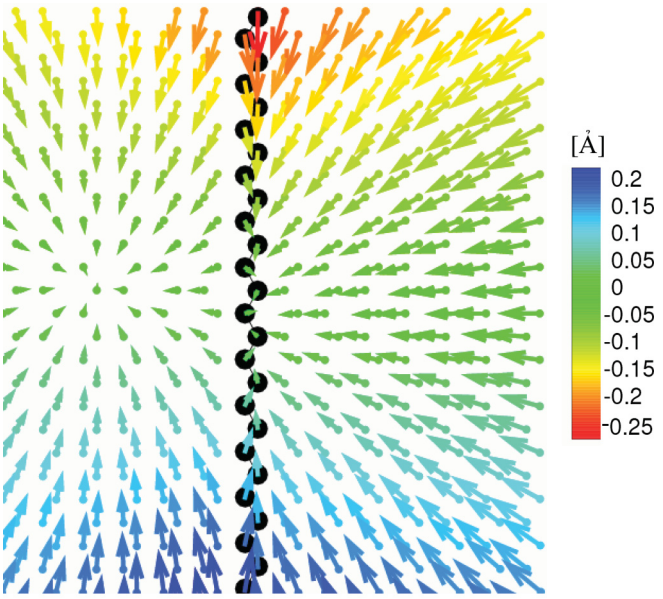

FIG. 4. (Color online) Atomic displacement after inserting an atomic carbon line in the middle of the BN sheet, i.e., NCB. The color coding indicates the y component of the displacement vector, i.e., red (blue) ≡ downward (upward) displacement.

and the passivation of the boundaries by H atoms lead to the appearance of a permanent dipole moment. For the case of BN [see Fig. 2(a)], using B3LYP we obtain a dipole moment $\vec{P_0} = (-10.58, -1.98)$ D [in this study, the electric-dipole moment vectors point from the negative charge to the positive charge, e.g., see red arrow in Fig. 2(a)], i.e., the system becomes piezoelectric. In the following, we investigate the influence of carbon doping on the polarization in BNNRs.

Inserting a C line alters the charge distribution mostly in the neighborhood of the C line (see Table I), while further away the charge distribution approaches that of a perfect BNNR. The different values of electronegativity for $B(\approx 2.0)$, $C(\approx 2.6)$, and $N(\approx 3.0)$ largely account for the charge redistribution and the concomitant formation of local dipoles.

For the NCB, the local dipoles for B-C and C-N bonds around the carbon line are directed to the right [Fig. 2(b)], which polarized NCB. Surprisingly, although local dipoles are in the x direction, we found that the total dipole moment is mainly in the y direction (parallel to the carbon line), i.e., using B3LYP we find $\vec{P_0} = (-9.37, -42.89)$D. We attribute this effect to the presence of carbon atoms in the middle of Fig. 2(b). The C atoms which are bonded to the B (N) atoms absorb (give) electronic charge yielding two different groups of C atoms, i.e., those bonded to B atoms with negative electronic charge and those bonded to N atoms with positive electronic charge. This is the main reason for the unusual direction of the dipole moment. In fact, the magnitude of P_y is related to the carbon line. Notice that this is seen only when different types of atoms surround the C line, i.e., the BCB and NCN systems have small P_x and P_y.

Notice that the dipole moment component parallel to the C line is one of the main results of our work and the other component (which is perpendicular to the C line) is

meaningless for the long ribbon. As can be seen from Fig. 3(b), a nonvanishing dipole moment, i.e., P_x, exists which is perpendicular to the C line. This component is partly due to the presence of the hydrogens at the edges and the nonrectangular shape of the flakes and it is also partly due to the carbon line. The former is eliminated for a long ribbon (see Fig. 10 for the BCCN system) or in the system which is periodically repeated along the ribbon axis.

As seen from Figs. 2(c) and 2(d) in the BCB and NCN systems, the dipoles of the left- and right-hand sides of the C line are in opposite directions and no overall dipole moment in the x direction arises from these edges. There is a small dipole moment P_y because the corners are differently terminated at the left and right edges.

A similar description is possible for the strong local dipoles on the B-C and N-C bonds induced by the insertion of the C line. Although having a C line in the middle, the BCB and NCN systems have vanishing dipole moments in the x direction because the local dipoles on the B-C and N-C bonds around the C line point in opposite directions. The direction of the local dipole moments, indicated by the horizontal black arrows in Figs. 2(b)–2(d), is chosen according to the electronegativity differences of the atoms as discussed earlier. It is important to note that the number and arrangement of hydrogen atoms are the same in all model systems, thus the main reason of the strong total polarization is the local arrangement of B and N atoms around the C line and not the presence of the H atoms at the edges.

D. Electrostatic potential

The electrostatic potential (ESP) mapped on the plane of the h-BN sheet for the representative models is shown in Fig. 5. The sign of ESP at any point depends on whether the ESP due to the nuclei and the electrons is dominant at that point. Figure 5(a) shows that the B-N bonds have a larger ESP (blue spots) around the B ions as compared to the N sites (red spots). It shows that the N ions attract electronic charge from the B ions as one expects in view of the atomic electronegativities. A characteristic pattern of alternating positive and negative ESP regions is seen over the BN surface in which the left side has generally less ESP than the right side. Accordingly, this explains why the BN has a permanent dipole moment in accordance of the electronegativity differences on H-B and H-N bonds at the edge which saturate the dangling bonds. The NCB, as shown in Fig. 5(b), has a steep gradient in the ESP near the C line which results in a strong dipole in this region and which confirms the direction of the dipole moment shown in Fig. 2(b). The big arrows in Figs. 5(a) and 5(b) refer to the dipole moments. Similarly, the direction of the opposite dipoles in Figs. 2(c) and 2(d) can be well explained by the ESP variation in Figs. 5(c) and 5(d). Strong variation of the ESP around the carbon lines causes strong dipoles but directed oppositely. In NCB, the antisymmetrical distribution is also due to the chosen nonperfect geometry of the corners.

E. Polarizability

The polarization of the BNNR system varies in response to an external electric field. Here, we focus on the NCB system

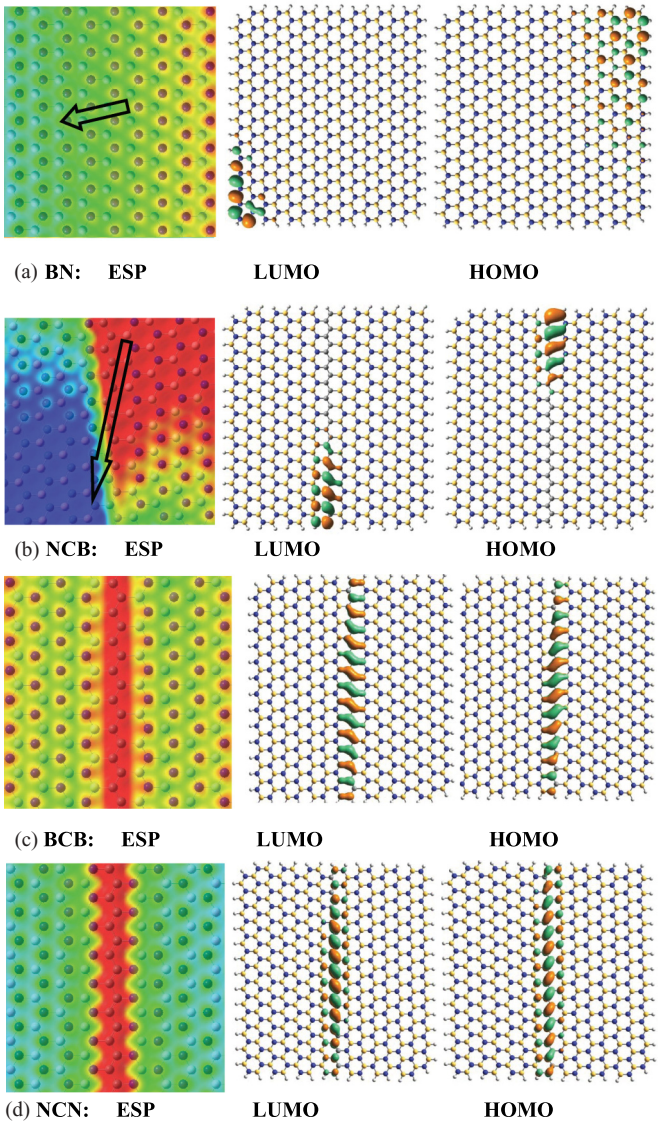

FIG. 5. (Color online) Contour plots of the electrostatic potential (ESP) projected on the sheet plane [regions with higher ESP are shown in blue ($\propto 1.5 \times 10^{-2}$ e) and regions with lower ESP in red ($\propto -1.5 \times 10^{-2}$ e)] and the corresponding HOMO and LUMO. In (a) and (b), the black arrows refer to the total dipole moment.

which has an appreciable permanent polarization. We apply a uniform electric field in the plane of the flakes parallel to the C line (y direction) and allow them to relax each time the electric field is altered. The reason for directing the field along y is that we want to compensate the largest component of the spontaneous dipole moment P_0, i.e., P_y. The field strength $E \equiv E_y$ is then increased stepwise until the induced dipole moment completely compensates P_y. We also inverted E_y to check the linear dependence. Red symbols in Fig. 6 (for the NCB system) show that the dipole moment has almost a linear dependence on E within the studied range $(-1.4, 0.8)$ V/nm. The slope of this line gives the polarizability $\alpha_{yy} = dE/dP_y$. From B3LYP we found $\alpha_{yy} = 45.66$ D nm/V and $E_0 \approx 1$ V/nm. In Figs. 6(b) and 6(c), we show the ESP and P_0 for $E_y = -1.0$ V/nm and $E_y = +0.82$ V/nm, respectively. The lattice deformations due to applied electric field are shown in Figs. 6(d) and 6(e). It

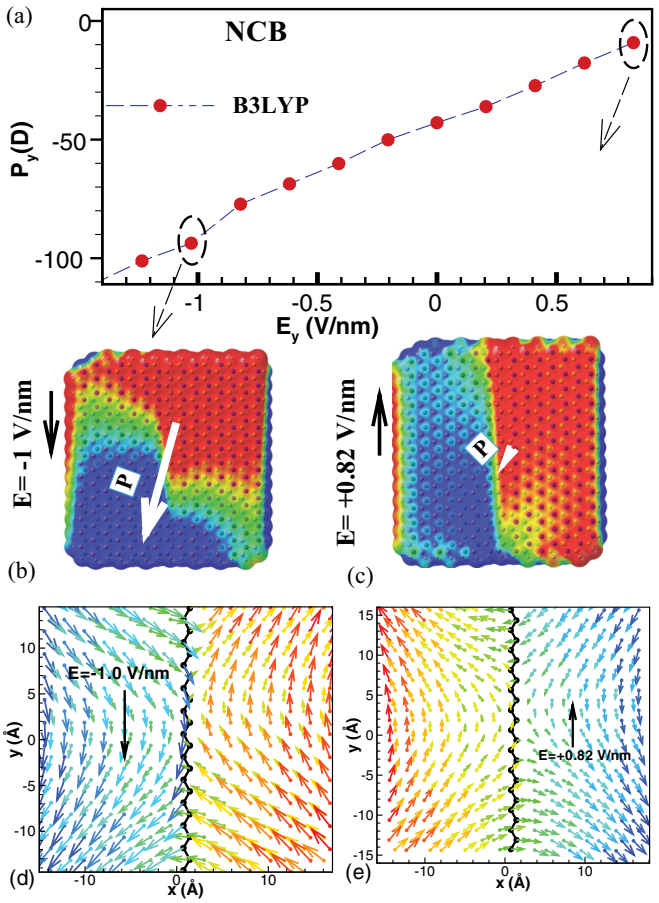

FIG. 6. (Color online) (a) Electric-dipole moment versus applied electric field, both in the y direction, for the NCB system using the B3LYP functional. The corresponding ESPs and lattice deformation for $E = E_y = -1.0$ V/nm [(b), (d)] and $E = E_y = +0.82$ V/nm [(c), (e)] [the color bars in (d) and (e) are the same as Fig. 4]. The black arrows (symbols) refer to the direction of the applied electric field (carbon atoms) and the white arrows refer to the total dipole moment.

is interesting to note that a positive electric field shifts the right-hand side atoms to the bottom and the left-hand side atoms to the top, and vice versa for the negative field. This yields a shear stress along the C line (filled black symbols). The larger the electric field, the larger the deformation and the larger the enhancement of piezoelectricity.

F. Metallic properties

To show the effect of the insertion of the C line on the conductivity of BNNRs, we have listed the calculated energy gaps for our systems in Table I. The gap is calculated as the energy difference between the highest occupied molecular orbital (HOMO) and the lowest unoccupied molecular orbital (LUMO). It is well known that LDA (which we used in our BIGDFT calculations) underestimates the energy of the excited levels and therefore the HOMO–LUMO gap, while the hybrid functional B3LYP is expected to give a better estimate. Both approximations (LDA/BIGDFT and B3LYP/Gaussian) reveal the same trend, i.e., significant decrease in the HOMO–LUMO gap after insertion of the C line. It implies that the electric conductivity is increased in the doped sheets, however, their gaps are still large and therefore the system is not metallic. We will show later that the HOMO–LUMO gap can also be tuned by an electric field. Figure 7 illustrates the density of states (DOS) for the studied BNNRs according to B3LYP. Note that the insertion of a C line generates a few new electronic states within the wide gap between the HOMO and LUMO of the perfect BN, reducing the gap width significantly. There are only few and well-separated energy levels below the HOMO of NCN and above the LUMO of BCB.

The change in the metallic properties can be explained by looking at the distribution of the electronic states near the Fermi level. As seen from Fig. 5, in the BN system the HOMO (LUMO) is localized at two corners around the N (B) atoms. In the BN system, the HOMO and LUMO are localized at the upper right- and the lower left-hand corners, respectively. It shows that both chirality and the local geometry of the edges are important parameters for localizing the electrons. On the other hand, in the doped systems the HOMO and LUMO states are localized around the C line over either B-C or N-C bonds [see Figs. 5(b) and 5(c)]. In BCB and NCN systems, the C line opens a wide channel of few atoms through which the electronic charge can be transmitted. But, the conductivity in the direction perpendicular to the C line is expected to be small

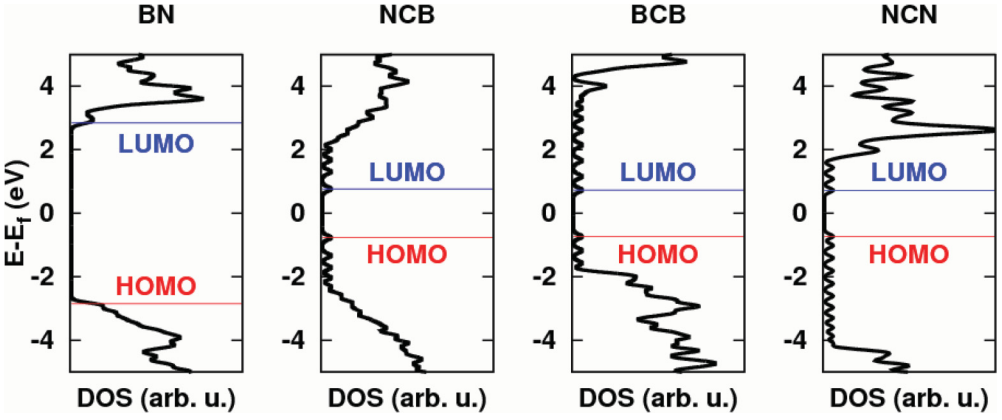

FIG. 7. (Color online) Density of states (DOS) for the four model systems. The presence of the carbon lines in the middle of the systems decreases the gap and modifies the DOS in different ways for each particular case.

because no contribution from HOMO and LUMO is extended along this direction. Notice that the localized orbitals in BCB and NCN have different patterns. In BCB, both HOMO and LUMO are localized on the C atoms and the adjacent B atoms (i.e., on the B-C bonds), while the N atoms are not contributing. In the NCN system, HOMO and LUMO are localized mainly on the C-C bonds (with different orientation for HOMO and LUMO) and are partially localized on the adjacent N atoms, and the B atoms never contribute.

The special shape of the localized HOMO and LUMO states around the two ends of the C line for the NCB is of most interest. The HOMO orbitals in NCB are localized over a few top C-C bonds and neighbor B atoms, while for the LUMO we notice that they are localized over a few bottom C-C bonds where B (N) atoms in the right-hand side (left-hand side partially) are mainly contributing with different shape as compared to the HOMO. It is important to emphasize that (i) we found the same orbital distribution in a BN system when it is doped by an armchair line of carbon atoms in the middle (those results are not reported in this paper), and (ii) we did not find such orbitals employing semi-infinite NCB, i.e., a ribbon with periodic boundary along the C line. The special shape of HOMO and LUMO orbitals found in NCB are not found in the BN system.[9,10]

Next, we will focus on the NCB system to study its response to an external electric field. When an electric field in the opposite direction of the dipole moment of the NCB is applied, the gap becomes smaller [see Fig. 8(a)], and the HOMO (LUMO) is localized much closer to the top (bottom) [see Fig. 8(c)]. On the other hand, we found in the previous section that the electric polarizability in response to an external field is increased by doping the BNNRs by carbon atoms. This trend can be used to obtain metallic properties in doped NCB. Insertion of different numbers of carbon lines as well as using different arrangements of the atoms near the C line can be a practical tool to tune the electric transmission through the BNNRs and their metallic properties.

An external uniform electric field E_y along the C line in NCB causes a potential difference along the C line. We assume that the HOMO and the LUMO are effectively centered around y_H and y_L, respectively. An applied electric field (E_y) can modulate the energy gap as $(y_L - y_H)e\,E_y$, where e is the elementary charge. The gap can be tuned by the strength and direction of the electric field. The latter linear behavior is obtained even using the LDA [see top inset in Fig. 8(a)] and is continued [with a slope of $(y_L - y_H)e$], while the centers of the HOMO and the LUMO are more or less fixed which is the case even for a rather strong field of $E = +0.82$ V/nm [compare Figs. 3(b) and 6(c)]. The same linear behavior is found for the reverse electric fields $E_y > -0.8$ V/nm [see Fig. 6(a)].

On the other hand, if a strong negative field of about -1 V/nm is applied, the dependence is no longer linear. Figure 6(b) shows that such a negative field alters the spatial distribution of the orbitals and elongates both HOMO and LUMO into a nonlocalized distribution similar to those found for the BCB or NCN systems. Therefore, around the maximum, $y_L \approx y_H$ and the energy gap is independent of the field strength. However, for the negative fields beyond the maximum, the energy gap decreases, which corresponds to the localization

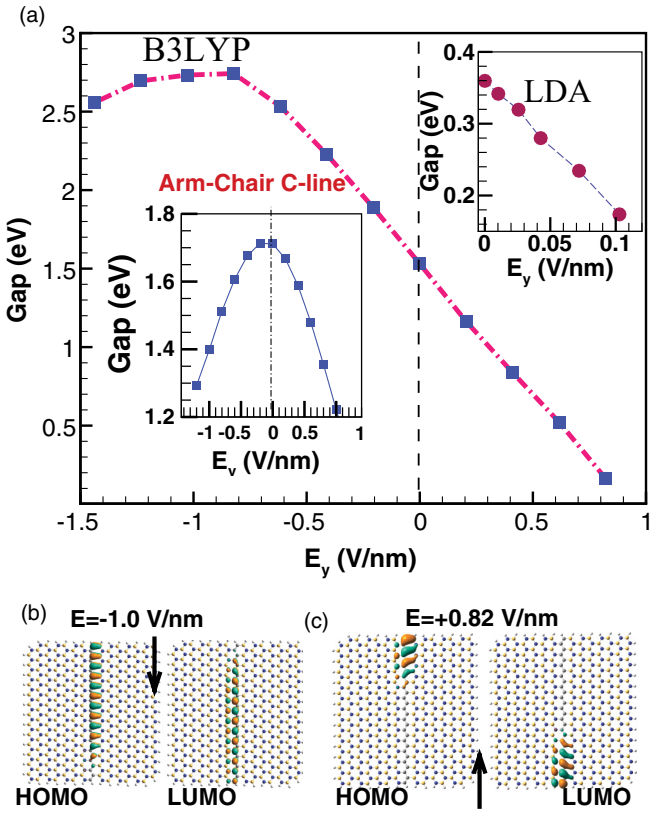

FIG. 8. (Color online) (a) The HOMO–LUMO energy gap for NCB versus applied electric field using B3LYP [and using LDA (top inset)]. Bottom inset shows the same quantity when an armchair line is replaced by C atoms. (b), (c) The shape of the HOMO and LUMO of NCB in the presence of electric fields of $E_y = -1.0$ V/nm (b) and $E_y = +0.82$ V/nm (c).

of the LUMO and the HOMO where $y_L < y_H$. This simple picture argues that $(y_L - y_H)e\,E_y$ modulates the energy gap. Notice that the slope $(y_L - y_H)e$ changes sign passing the maximum ($E_y \simeq -1$ V/nm), therefore, by decreasing the electric field, the gap decreases when $E_y \geqslant -1$ V/nm and increases when $E_y \leqslant -1$ V/nm. A similar behavior was found for semi-infinite nondoped BN systems,[9,10] but with a difference in maximum and energy-gap values. The bottom inset in Fig. 6(a) shows the variation of the HOMO and LUMO states with the electric field. The band gap is one of the key factors that characterizes the electronic transport (but not the only one). We showed that the energy gap of the NCB system can be controlled well with a external field. Such a system might therefore be of great practical interest.

G. Effect of the size

In order to study the effect of the nanoribbon width, we performed further calculations for the BCN arrangement with two smaller widths, i.e., $W = 2.27$ and 1.35 nm. The corresponding ESPs and HOMO and LUMO distributions are shown in Fig. 9, which are similar to those of the BCN with a width of $W = 3.4$ nm [cf. Fig. 5(b)]. Therefore, the most important features, i.e., the localization of the molecular orbitals at the ends of the C line as well as the strong polarization along the C line are size independent. The dipole moment is reduced

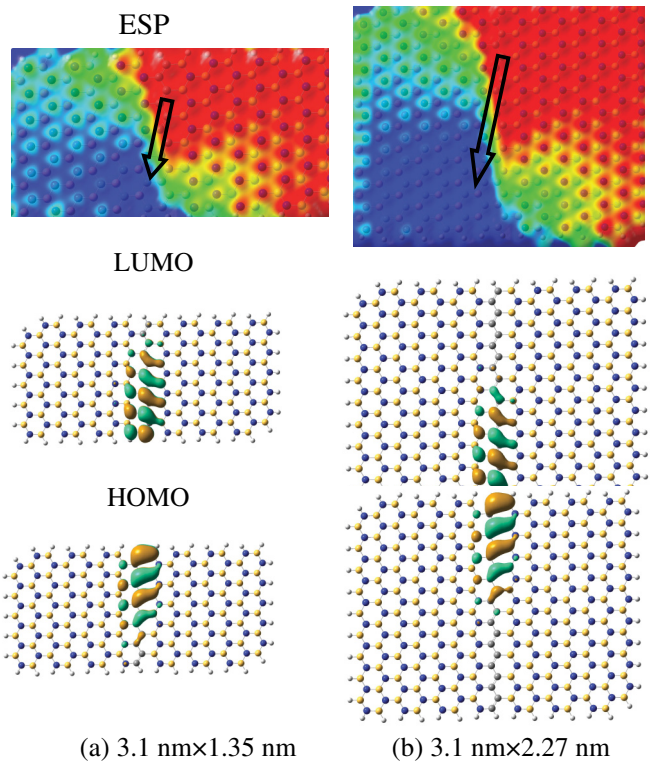

FIG. 9. (Color online) ESP projected on the sheet plane (regions with higher ESP are shown in blue and regions with lower ESP in red) and HOMO and LUMO for two BCN systems with $W = 1.35$ nm (a) and $W = 2.27$ nm (b).

by decreasing the width W of the nanoribbon (see Table II). This is expected because the dipole moment, by definition, is proportional to the separation between the positively charged region (which is mostly concentrated at the bottom edges as seen from ESPs) and the negatively charged part (i.e., the top edges). Furthermore, the energy gap increases with decreasing width, which is due to the fact that increasing of the number of carbon atoms brings along electronic states with energies located within the band gap.

H. Armchair carbon line

In this section, we compare the electronic properties of a BN sheet doped with an armchair C line in the middle with that of a zigzag C line in the middle. There are two different ways of inserting an armchair C line in the middle of a BN sheet, i.e., the atomic arrangement on successive zigzag lines is (i) BCCN and NCCB [see Fig. 10(a)] or (ii) BCCB and NCCN [see Fig. 11(a)]. The response of zigzag and armchair C lines to the external electric field is also different. The corresponding

TABLE II. The effect of the size (width) on the energy gap and dipole moment for the BCN arrangement.

W (nm)	Gap (eV)	P_o (D)
3.46	1.52	44.24
2.27	1.87	27.65
1.35	2.51	17.93

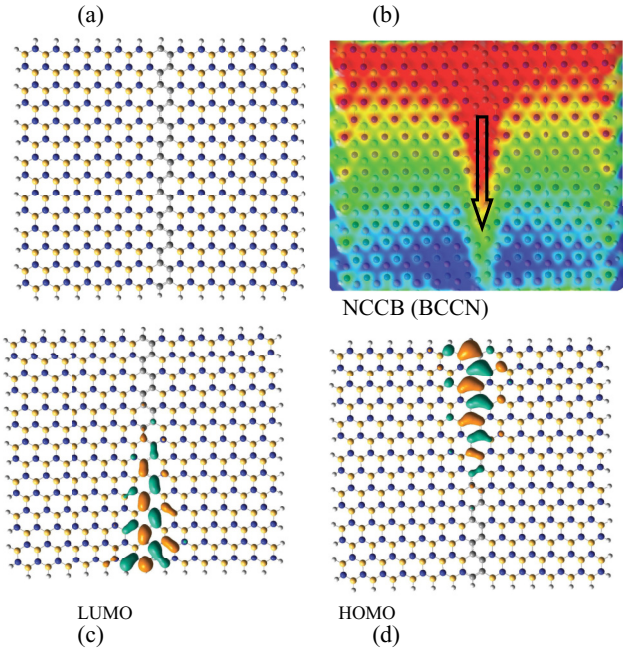

FIG. 10. (Color online) BN sheet doped with an armchair carbon line (a) and the corresponding ESP (b), LUMO (c), and HOMO (d) where the atomic arrangement on successive zigzag lines is NCCB (or BCCN).

ESPs, LUMO, and HOMO are depicted in Figs. 10(b)–10(d) and 11(b)–11(d), respectively. Although, the ESPs around the armchair C line [Figs. 10(b) and 11(b)] are completely different

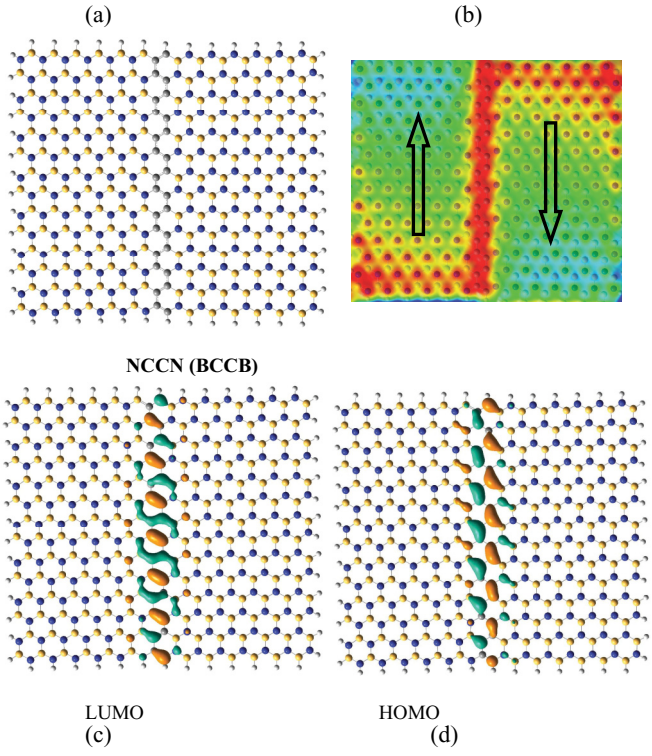

FIG. 11. (Color online) BN sheet doped with an armchair carbon line (a) and the corresponding ESP (b), LUMO (c), and HOMO (d) where the atomic arrangement on successive zigzag lines is BCCB and NCCN.

from that around the zigzag C line (Fig. 5), however, localized molecular orbitals around the C line appear in all cases. For the armchair-doped BN sheet, only the arrangement BCCN has separated HOMO and LUMO at the two ends of the C line, hence, the gap is tunable by applying an electric field along the C line. The inset in Fig. 8 shows the variation of the energy gap with electric field for the BN sheet with an armchair C line in the middle. On the other hand, the BCCB arrangement possesses a large dipole moment but exhibits less sensitivity of the gap to the applied electric field.

IV. CONCLUSIONS

In summary, we studied the electronic properties of boron nitride sheets in the presence of a zigzag or armchair atomic line of carbon atoms in the middle of the sheets. Electronic polarization of the BNNRs was found to depend on the local arrangement of the boron and nitrogen atoms around the carbon line. Doping with carbon atoms decreases the nonmetallic feature of the BNNRs by reducing the energy gap and increasing the polarizability. We showed that for different widths of the BNNR and in both zigzag and armchair directions, doping the BNNR with a carbon line has a major impact on the spatial distribution of the molecular orbitals close to the Fermi level as well as on their energies. By applying an electric field along the carbon line, we showed that the dipole moment of BNNR induced by the carbon dopant can be reduced and even eliminated. This also reduces the energy gap in the energy spectrum and allows one to control the conductivity with an external field. The energy gap is underestimated by LDA as compared to the B3LYP hybrid functional, but the decreasing trend of the energy gap of the BN system due to the insertion of the C line is qualitatively similar.

ACKNOWLEDGMENTS

We would like to thank J. M. Pereira and S. Goedecker for helpful discussions. This work was supported by the Flemish Science Foundation (FWO-Vl), the ESF-EuroGRAPHENE project CONGRAN. M.N.-A is supported by EU-Marie Curie IIF postdoc Fellowship/299522.

*Corresponding author: neekamal@srttu.edu

[1]D. Pacile, J. C. Meyer, C. O. Girit, and A. Zettl, Appl. Phys. Lett. **92**, 133107 (2008).
[2]C. H. Jin, F. Lin, K. Suenaga, and S. Iijima, Phys. Rev. Lett. **102**, 195505 (2009).
[3]J. C. Meyer, A. Chuvilin, G. Algara-Siller, J. Biskupek, and U. Kaiser, Nano Lett. **9**, 2683 (2009).
[4]X. Blase, A. Rubio, S. G. Louie, and M. L. Cohen, Phys. Rev. B **51**, 6868 (1995).
[5]K. Watanabe, T. Taniguchi, and H. Kanda, Nat. Mater. **3**, 404 (2004).
[6]Liam Britnell, Roman V. Gorbachev, Rashid Jalil, Branson D. Belle, Fred Schedin, Mikhail I. Katsnelson, Laurence Eaves, Sergey V. Morozov, Alexander S. Mayorov, Nuno M. R. Peres, Antonio H. Castro Neto, Jon Leist, Andre K. Geim, Leonid A. Ponomarenko, and Kostya S. Novoselov, Nano Lett. **12**, 1707 (2012).
[7]G-H. Lee, Y-J. Yu, C. Lee, C. Dean, K. L. Shepard, P. Kim, and J. Hone, Appl. Phys. Lett. **99**, 243114 (2011).
[8]W. Chen, Y. Li, G. Yu, Z. Zhou, and Z. Chen, J. Chem. Theory Comput. **5**, 3088 (2009).
[9]C. H. Park and S. G. Louie, Nano Lett. **8**, 2200 (2008).
[10]Z. Zhang and W. Guo, Phys. Rev. B **77**, 075403 (2008).
[11]F. Zheng, G. Zhou, Z. Liu, J. Wu, W. Duan, B.-L. Gu, and S. B. Zhang, Phys. Rev. B **78**, 205415 (2008).
[12]L. Lai, J. Lu, L. Wang, G. Luo, J. Zhou, R. Qin, Z. Gao, and W. N. Mei, J. Phys. Chem. C **113**, 2273 (2009).
[13]Y. Wang, Y. Ding, and J. Ni, Phys. Rev. B **81**, 193407 (2010).
[14]Y. Ding, Y. Wang, and J. Ni, Appl. Phys. Lett. **94**, 233107 (2009).
[15]L. Ci, L. Song, C. Jin, D. Jariwala, D. Wu, Y. Li, A. Srivastava, Z. F. Wang, K. Storr, L. Balicas, F. Liu, and P. M. Ajayan, Nat. Mater. **9**, 430 (2010).
[16]M. Chen, Y-J. Zhao, J-H. Liao, and X-B. Yang, Phys. Rev. B **86**, 045459 (2012).
[17]A. J. Du, S. C. Smith, and G. Q. Lu, Chem. Phys. Lett. **447**, 181 (2007).
[18]R. Q. Wu, L. Liu, G. W. Peng, and Y. P. Feng, Appl. Phys. Lett. **86**, 122510 (2005).
[19]N. Sai and E. J. Mele, Phys. Rev. B **68**, 241405 (2003).
[20]M. J. Frisch *et al.*, GAUSSIAN 1998, http://www.gaussian.com/.
[21]L. Genovese, A. Neelov, S. Goedecker, T. Deutsch, S. A. Ghasemi, A. Willand, D. Caliste, O. Zilberberg, M. Rayson, A. Bergman, and R. Schneider, J. Chem. Phys. **129**, 014109 (2008).
[22]A. Reed, L. Curtiss, and F. Weinhold, Chem. Rev. **88**, 899 (1988).
[23]R. S. Pease, Acta. Crystallogr. **5**, 356 (1952).
[24]G. Kern, G. Kresse, and J. Hafner, Phys. Rev. B **59**, 8551 (1999).
[25]K. H. Michel and B. Verberck, Phys. Rev. B **80**, 224301 (2009).
[26]K. H. Michel and B. Verberck, Phys. Rev. B **83**, 115328 (2011).